Bol. Soc. Paran. Mat.
©SPM –ISSN-2175-1188 ON LINE
SPM: www.spm.uem.br/bspm

(3s.) **v. 38** 2 (2020): 61–74.
ISSN-00378712 IN PRESS
doi:10.5269/bspm.v38i2.38043

Convergence of Approximate Solution of Mixed Hammerstein Type Integral Equations

Monireh Nosrati Sahlan

ABSTRACT: In the present paper, a computational method for solving nonlinear Volterra-Fredholm Hammerstein integral equations is proposed by using compactly supported semiorthogonal cubic B-spline wavelets as basis functions. Dual functions and Operational matrices of B-spline wavelets via Galerkin method are utilized to reduce the computation of integral equations to some algebraic system, where in the Galerkin method dual of B-spline wavelets are applied as weighting functions. The method is computationally attractive, and applications are demonstrated through illustrative examples.

Key Words: Hammerstein integral equations, Cubic B-spline wavelets, Operational matrices, Galerkin method, Error analysis.

Contents

1. Introduction

The past two decades have been witnessing a strong interest among physicists, engineers and mathematicians for the theory and numerical modeling of integral equations. These equations are solved analytically; for example in [1] and the references therein. Although proving existence and uniqueness of solution of integral equation has been done lots of researches [2]- [5], but analytical solutions for those often are not available. Nonlinear integral equations have been studied in relation to physics, vehicular traffic, biology, the theory of optimal control, economics, etc. Several numerical methods for approximating the solution of mixed Volterra-Fredholm Hammerstein integral equations are known. In [6] a direct method based on new

2010 *Mathematics Subject Classification:* 45G10, 65L60, 42C40, 65Gxx.
Submitted July 08, 2017. Published October 02, 2017

basis functions, derived from Block-Pulse functions, is presented for solving nonlinear type of these equations. Two dimensional mixed Volterra-Fredholm integral equations of Urysohn type are solved by using some meshless methods in [7], and variational iteration method in [8]. Also the numerical solution of Hammerstein integral equations of mixed type by using Sinc-collocation method was introduced in [9]. The methods in [10]- [13] transform a given integral equation into a system of nonlinear equations, which has to be solved with some kind of an iterative method.
Consider the second kind nonlinear Fredholm-Volterra-Hammerstein integral equation of the form

$$y(x) = f(x) + \int_0^1 K_1(x,t)g_1(t,y(t))dt + \int_0^x K_2(x,t)g_2(t,y(t))dt, \qquad (1.1)$$
$$0 \le x,t \le 1,$$

where f, K_1 and K_2 are known L^2 functions, with $g_1(t,y(t))$ and $g_2(t,y(t))$ nonlinear in y, the unknown function that to be determined.
In this paper, we use the semiorthogonal cubic B-spline wavelets for solving this class of integral equations. Our method consists of reducing the given mixed integral equation to a set of algebraic equations by expanding the unknown function by B-spline wavelets with unknown coefficients. Operational matrices via Galerkin method are utilized to evaluate the unknown coefficients. Because of semiorthogonality, having compact support and vanishing moments properties of these wavelets, the operational matrices are very sparse.
The structure of this paper is arranged as follows. The main problem and brief history of some presented methods are expressed in section 1. Section 2 is devoted to definition of cubic B-spline wavelets on bounded interval, function approximation by using these wavelets and dual of cubic B-spline scaling functions and wavelets. In section 3, the numerical method for solving Volterra-Fredholm Hammerstein integral equation is purposed. In section 4 convergence and error analysis of the method are discussed. In section 5, we report our numerical founds and compare them with some other methods in solving these integral equations, and section 6 contains our conclusion.

2. Cubic B-spline scaling and wavelet functions

The general theory and basic concepts of the wavelet theory and MRA is given in [14]- [19]. There are several ways to define B-splines. Typically, the $m-$th order B-splines $\varphi_m(t)$ is defined recursively by convolution

$$\varphi_1(t) = \chi_{[0,1]}(t), \qquad (2.1)$$
$$\varphi_m(t) = \int_{-\infty}^{\infty} \varphi_{m-1}(t-x)\varphi_1(x)dx = \int_0^1 \varphi_{m-1}(t-x)dx. \qquad (2.2)$$

Another recursive relation for B-spline scaling functions of order $m \ge 2$ is as follows

$$\varphi_m(t) = \frac{t}{m-1}\varphi_{m-1}(t) + \frac{m-t}{m-1}\varphi_{m-1}(t-1), \qquad (2.3)$$

and supp $\varphi_m = [0, m]$. Cubic B-Spline $\varphi_4(x)$ is derived from the recurrence (2.1) and (2.2) as the case of $m = 4$ for general B-splines as follows [11]

$$\varphi_4(x) = \frac{1}{6}\begin{cases} x^3 & x \in [0,1) \\ -3x^3 + 12x^2 - 12x + 4 & x \in [1,2) \\ 3x^3 - 24x^2 + 60x - 44 & x \in [2,3) \\ (4-x)^3 & x \in [3,4) \\ 0 & otherwise, \end{cases}$$

or in the other form

$$\varphi_4(x) = \left(\frac{1}{6}\sum_{k=0}^{4}\binom{4}{k}(-1)^k(x-k)_+^3\right)\chi_{[0,4]}(x), \tag{2.4}$$

where

$$x_+^n = \begin{cases} x^n & , x > 0 \\ 0 & , x \le 0. \end{cases}$$

and its *two-scale dilation equation* defined as follows

$$\varphi_4(x) = \sum_{k=0}^{4}\frac{1}{8}\binom{4}{k}\varphi_4(2x-k).$$

Scaling functions can be used to expand any function in $L^2(\mathbb{R})$. These functions are defined on the entire real lines, so that they could be outside of the domain of the problem. The common strategy is to use as many translates as possible of the generators supported inside the interval $[0, 1]$ and construct boundary functions for those generators that overlap the interval end. The construction will be done on a minimal level J which is chosen such that the boundary functions on the right and on the left do not overlap. In that way both ends of the interval can be treated separately. In our setting this is satisfied for $J \ge 3$.

Boundary adaptation

- Left boundary cubic B-spline scaling functions:
  We define the boundary near functions at the left boundary by

  $$\phi_{3,k}(x) = \varphi_4(8x-k)\chi_{[0,1]}(x), \qquad k = -3, -2, -1, \tag{2.5}$$

  and for other levels of J, we have

  $$\phi_{J,k}(x) = \varphi_4(2^J x - k)\chi_{[0,1]}(x), \quad k = -3, -2, -1, \quad J = 4, 5, \ldots. \tag{2.6}$$

- Right boundary cubic B-spline scaling functions:
  For the right end of the interval, note that, by symmetry we have the following relations

  $$\phi_{3,5}(x) = \phi_{3,-1}(1-x), \tag{2.7}$$

$$\phi_{3,6}(x) = \phi_{3,-2}(1-x), \tag{2.8}$$
$$\phi_{3,7}(x) = \phi_{3,-3}(1-x), \tag{2.9}$$

and for other levels of J, we have

$$\phi_{J,2^J-k-3}(x) = \phi_{3,k}(2^J x - k), \quad k = -3,-2,-1, \quad J = 4,5,\ldots. \tag{2.10}$$

Interior scalings

Five interior cubic B-spline scaling functions are chosen as

$$\phi_{3,k}(x) = \varphi_4(8x-k)\chi_{[0,1]}(x), \quad k = 0,1,2,3,4, \tag{2.11}$$

and for other levels of J, we get

$$\phi_{J,k}(x) = \varphi_4(2^J x - k)\chi_{[0,1]}(x), \quad k = 0,1,...,2^J-4, \quad J = 4,5,\ldots. \tag{2.12}$$

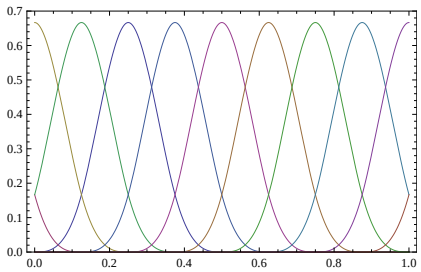

Figure 1: Inner and boundary cubic B-spline scaling functions

Two scale delation equation for cubic B-spline wavelet is given by:

$$\psi_4(x) = \sum_{k=0}^{10} \frac{(-1)^k}{8} \sum_{l=0}^{4} \begin{pmatrix} 4 \\ l \end{pmatrix} \varphi_8(k-l+1)\varphi_4(2x-k). \tag{2.13}$$

Other inner and boundary wavelets are made similarly [20]. Figure 3 is helpful to get a geometric understanding of inner and boundary cubic B-spline wavelets.

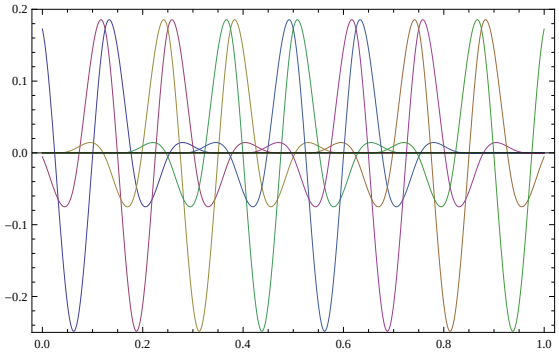

Figure 2: Cubic B-spline inner and boundary wavelets.

2.1. Function approximation

A function $f(x)$ defined over $[0,1]$ may be approximated by cubic B-spline wavelets as

$$f(x) = \sum_{i=-3}^{2^{j_0}-1} c_{j_0,i}\phi_{j_0,i}(x) + \sum_{j=j_0}^{\infty}\sum_{k=-3}^{2^j-4} d_{j,k}\psi_{j,k}(x), \tag{2.14}$$

where $\phi_{j_0,i}$ and $\psi_{j,k}$ are scaling and wavelets functions, respectively. If the infinite series in equation (2.14) is truncated, then it can be written as

$$f(x) \simeq \sum_{i=-3}^{2^{j_0}-1} c_{j_0,i}\phi_{j_0,i}(x) + \sum_{j=j_0}^{j_u}\sum_{k=-3}^{2^j-4} d_{j,k}\psi_{j,k}(x) = C^T\Upsilon(x), \tag{2.15}$$

where C and Υ are $2^{(j_u+1)}+3$ column vectors given by

$$C = \left(c_{j_0,-3},...,c_{j_0,2^{j_0}-1},d_{j_0,-3},...,d_{j_0,2^{j_0}-4},...,d_{j_u,-3},...,d_{j_u,2^{j_u}-4}\right)^T, \tag{2.16}$$

$$\Upsilon = \left(\phi_{j_0,-3},...,\phi_{j_0,2^{j_0}-1},\psi_{j_0,-3},...,\psi_{j_0,2^{j_0}-4},...,\psi_{j_u,-3},...,\psi_{j_u,2^{j_u}-4}\right)^T, \tag{2.17}$$

with

$$c_{j_0,i} = \int_0^1 f(x)\tilde{\phi}_{j_0,i}(x)dx \quad , \quad i = -3,...,2^{j_0}-1,$$

$$d_{j,k} = \int_0^1 f(x)\tilde{\psi}_{j,k}(x)dx \quad , \quad j = j_0,...,j_u \ , \ k = -3,...,2^{j_u}-4,$$

and $\tilde{\varphi}_{j_0,i}$ and $\tilde{\psi}_{j,k}$ are dual functions of $\varphi_{j_0,i}, i = -3,...,2^{j_0}-1$ and $\psi_{j,k}, j = j_0,...,j_u,\ k = -3,...,2^j-4$, respectively. These can be obtained by linear combinations of $\varphi^{(3)}_{j_0,i}$ and $\psi_{j,k}$. Let

$$\phi(x) = \left(\phi_{j_0,-3}(x),\phi_{j_0,-2}(x),...,\phi_{j_0,7}(x)\right)^T, \tag{2.18}$$

$$\psi(x) = \left(\psi_{3,-3}(x),...,\psi_{3,4}(x),...,\psi^{()}_{j_u,2^{j_u}-4}(x)\right)^T. \tag{2.19}$$

Using equations (2.18)-(2.19) we get

$$\int_0^1 \varphi(x)\varphi^T(x)dx = P_1, \tag{2.20}$$

where

$$P_1 = \begin{pmatrix} \frac{1}{2016} & \frac{43}{13440} & \frac{1}{672} & \frac{1}{40320} & 0 & 0 & 0 & 0 & 0 & 0 & 0 \\ \frac{43}{13440} & \frac{151}{5040} & \frac{59}{2240} & \frac{1}{336} & \frac{1}{40320} & 0 & 0 & 0 & 0 & 0 & 0 \\ \frac{1}{672} & \frac{59}{2240} & \frac{599}{10080} & \frac{397}{13440} & \frac{1}{336} & \frac{1}{40320} & 0 & 0 & 0 & 0 & 0 \\ \frac{1}{40320} & \frac{1}{336} & \frac{397}{13440} & \frac{151}{2520} & \frac{397}{13440} & \frac{1}{336} & \frac{1}{40320} & 0 & 0 & 0 & 0 \\ 0 & \frac{1}{40320} & \frac{1}{336} & \frac{397}{13440} & \frac{151}{2520} & \frac{397}{13440} & \frac{1}{336} & \frac{1}{40320} & 0 & 0 & 0 \\ 0 & 0 & \frac{1}{40320} & \frac{1}{336} & \frac{397}{13440} & \frac{151}{2520} & \frac{397}{13440} & \frac{1}{336} & \frac{1}{40320} & 0 & 0 \\ 0 & 0 & 0 & \frac{1}{40320} & \frac{1}{336} & \frac{397}{13440} & \frac{151}{2520} & \frac{397}{13440} & \frac{1}{336} & \frac{1}{40320} & 0 \\ 0 & 0 & 0 & 0 & \frac{1}{40320} & \frac{1}{336} & \frac{397}{13440} & \frac{151}{2520} & \frac{397}{13440} & \frac{1}{336} & \frac{1}{40320} \\ 0 & 0 & 0 & 0 & 0 & \frac{1}{40320} & \frac{1}{336} & \frac{397}{13440} & \frac{599}{10800} & \frac{59}{2240} & \frac{1}{672} \\ 0 & 0 & 0 & 0 & 0 & 0 & \frac{1}{40320} & \frac{1}{336} & \frac{59}{2240} & \frac{151}{5040} & \frac{43}{13440} \\ 0 & 0 & 0 & 0 & 0 & 0 & 0 & \frac{1}{40320} & \frac{1}{672} & \frac{43}{13440} & \frac{1}{2016} \end{pmatrix},$$

Figure 3: Inner and boundary cubic B-spline scaling functions

similarly for cubic B-spline wavelets, product matrix is:

$$\int_0^1 \psi(x)\psi^T(x)dx = P_2 = \begin{pmatrix} H_{8\times 8} & & & \\ & \frac{1}{2}H_{16\times 16} & & \\ & & \ddots & \\ & & & \frac{1}{2^{j_u-3}}H_{2^{j_u}\times 2^{j_u}} \end{pmatrix}, \quad (2.21)$$

where P_1 and P_2 are 11×11 and $(2^{j_u+1}-8) \times (2^{j_u+1}-8)$ matrices, respectively. For $j_u = 3$, $H_{8\times 8}$ is as follows

$$H_{8\times 8} = \begin{pmatrix} \frac{402}{100000} & \frac{14}{10000} & \frac{-59}{100000} & \frac{-8}{100000} & 0 & 0 & 0 & 0 \\ \frac{14}{10000} & \frac{52}{10000} & \frac{14}{10000} & \frac{-59}{100000} & \frac{-8}{100000} & 0 & 0 & 0 \\ \frac{-59}{100000} & \frac{14}{10000} & \frac{52}{10000} & \frac{14}{10000} & \frac{-59}{100000} & \frac{-8}{100000} & 0 & 0 \\ \frac{-8}{100000} & \frac{-59}{100000} & \frac{14}{10000} & \frac{52}{10000} & \frac{15}{10000} & \frac{-59}{100000} & \frac{-8}{100000} & 0 \\ 0 & \frac{-8}{100000} & \frac{-59}{100000} & \frac{15}{10000} & \frac{52}{10000} & \frac{14}{10000} & \frac{-59}{100000} & \frac{-8}{100000} \\ 0 & 0 & \frac{-8}{100000} & \frac{-59}{100000} & \frac{14}{10000} & \frac{52}{10000} & \frac{14}{10000} & \frac{-59}{100000} \\ 0 & 0 & 0 & \frac{-8}{100000} & \frac{-59}{100000} & \frac{14}{10000} & \frac{52}{10000} & \frac{14}{10000} \\ 0 & 0 & 0 & 0 & \frac{-8}{100000} & \frac{-59}{100000} & \frac{14}{10000} & \frac{402}{100000} \end{pmatrix}$$

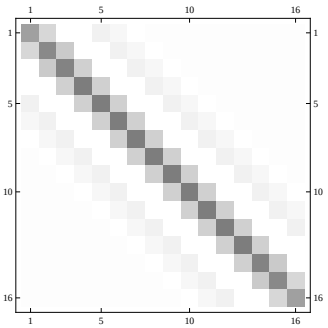

Figure 4: Graylevel matrix of the $H_{16\times 16}$

In greyscale plot of matrix, a darker color on an element indicates a larger magnitude. As is shown in the Figure 3, the product matrix of wavelet functions is very sparse because of semiorthogonality, compact support properties of cubic B-spline wavelet functions.
Suppose $\tilde{\varphi}(x)$ and $\tilde{\psi}(x)$ are the dual functions of $\varphi(x)$ and $\psi(x)$, respectively, given by

$$\tilde{\phi}(x) = [\tilde{\phi}^{(3)}_{4,-3}(x), \tilde{\phi}^{(3)}_{4,-2}(x), ..., \tilde{\phi}^{(3)}_{4,7}(x)]^T, \tag{2.22}$$

$$\tilde{\psi}(x) = [\tilde{\psi}^{(3)}_{4,-3}(x), ..., \tilde{\psi}^{(3)}_{4,4}(x), ..., \tilde{\psi}^{(j_u)}_{4,2^{j_u}-4}(x)]^T. \tag{2.23}$$

Using (2.18)-(2.23) we get

$$\int_0^1 \tilde{\varphi}(x)\varphi^T(x)dx = I_{11}, \quad \int_0^1 \tilde{\psi}(x)\psi^T(x)dx = I_{2^{j_u+1}-8}.$$

where I_{11} and $I_{2^{j_u+1}-8}$ are 11×11 and $(2^{j_u+1}-8) \times (2^{j_u+1}-8)$ identity matrices, respectively.
Thus we get

$$\tilde{\varphi} = P_1^{-1}\varphi, \qquad \tilde{\psi} = P_2^{-1}\psi.$$

3. Wavelet Galerkin Method for solving mixed integral equations

In this section, we solve the integral equation of the form (1) by using operational matrix of cubic B-spline wavelets. The unknown functions in equation (1.1) can be expanded in term of the selected scaling and wavelet functions as equation (2.15)

$$y(x) = C^T\Upsilon(x), \tag{3.1}$$

$$g_1(x, y(x)) = Z_1(x) = A_1^T\Upsilon(x), \tag{3.2}$$

$$g_2(x, y(x)) = Z_2(x) = A_2^T\Upsilon(x), \tag{3.3}$$

where $\Upsilon(x)$ is defined in (2.17) and C, A_1 and A_2 are $(2^{j_u+1}+3)\times 1$ unknown vectors defined similarly C in (2.16). The known functions in equation (1.1), $f(x), K_1(x,t)$ and $K_2(x,t)$, can be expanded by B-spline dual wavelets $\widetilde{\Upsilon}$ given by

$$\widetilde{\Upsilon} = \left(\widetilde{\varphi}^{(3)}_{j_0,-3}, ..., \widetilde{\varphi}^{(3)}_{j_0,2^{j_0}-1}, \widetilde{\psi}_{j_0,-3}, ..., \widetilde{\psi}_{j_0,2^{j_0}-4}, ..., \widetilde{\psi}_{j_u,-3}, ..., \widetilde{\psi}_{j_u,2^{j_u}-4}\right)^T, \tag{3.4}$$

that is

$$f(x) = D^T\widetilde{\Upsilon}(x), \tag{3.5}$$

$$K_1(x,t) = \widetilde{\Upsilon}^T(t)E_1\widetilde{\Upsilon}(x), \tag{3.6}$$

$$K_2(x,t) = \widetilde{\Upsilon}^T(t)E_2\widetilde{\Upsilon}(x), \tag{3.7}$$

where

$$E_l = \left(\int_0^1 \left(\int_0^1 K_l(x,t)\Upsilon_i(t)dt\right)\Upsilon_j(x)dx\right)_{i,j},$$

$$l = 1, 2, \quad i, j = 1, 2, ..., 2^{j_u+1} + 3,$$

and Υ_i is the $i-th$ element of the column vector Υ. Using equations (3.2)-(3.3) and (3.6)-(3.7) we get

$$\int_0^1 K_1(x,t)g_1(t,y(t))dt = \int_0^1 A_1^T \Upsilon(t)\widetilde{\Upsilon}^T(t)E_1\widetilde{\Upsilon}(x)dt = A_1^T E_1 \widetilde{\Upsilon}(x), \tag{3.8}$$

$$\int_0^1 K_2(x,t)g_2(t,y(t))dt = \int_0^x A_2^T \Upsilon(t)\widetilde{\Upsilon}^T(t)E_2\widetilde{\Upsilon}(x)dt = A_2^T P_x E_2 \widetilde{\Upsilon}(x), \tag{3.9}$$

and P_x is functional matrix defined as

$$P_x = \int_0^x \Upsilon(t)\widetilde{\Upsilon}^T(t)dt$$

By substituting (3.1), (3.5) and (3.8)-(3.9) in equation (1.1), we have

$$C^T\Upsilon(x) = D^T\widetilde{\Upsilon}(x) + A_1^T E_1\widetilde{\Upsilon}(x) + A_2^T P_x E_2\widetilde{\Upsilon}(x), \tag{3.10}$$

by multiplying (3.10) by $\Upsilon^T(x)$ and integrating from 0 to 1, we get

$$C^T \int_0^1 \Upsilon(x)\Upsilon^T(x)dx = D^T \int_0^1 \Upsilon^T(x)\widetilde{\Upsilon}(x)dx + A_1^T E_1 \int_0^1 \Upsilon^T(x)\widetilde{\Upsilon}(x)dx$$
$$+ A_2^T \int_0^1 \Upsilon^T(x)P_x E_2\widetilde{\Upsilon}(x)dx, \tag{3.11}$$

therefore

$$C^T P = D^T + A_1^T E_1 + A_2^T \Lambda, \tag{3.12}$$

in which P is a $(2^{j_u+1}+3)\times(2^{j_u+1}+3)$ square matrix given by

$$P = \begin{pmatrix} P_1 & \\ & P_2 \end{pmatrix},$$

where P_1 and P_2 are defined in equations (2.20)-(2.21), and

$$\Lambda = \int_0^1 \Upsilon^T(x)P_x E_2\widetilde{\Upsilon}(x)dx.$$

To find the solution $y(x)$, we first collocate the following equations

$$g_1(x, C^T\Upsilon(x)) = A_1^T\Upsilon(x), \tag{3.13}$$

$$g_2(x, C^T\Upsilon(x)) = A_2^T\Upsilon(x), \tag{3.14}$$

in the collocation points

$$x_m = \frac{m}{2^{(j_u+1)}+3}, \quad m = 1, 2, ..., 2^{(j_u+1)}+3,$$

equation (3.12) generates a set of $2\times(2^{j_u+1}+3)$ algebraic equations. The total number of unknowns for vectors C, A_1 and A_2 in equation (3.12) is $3\times(2^{j_u+1}+3)$. These can be obtained by using equations (3.13) and (3.14).

4. Convergence and error estimate

In this section, we discuss about convergence and error bounds of introduced method and by recalling some relevant theorems, we prove the main theorem of this paper.

Theorem 4.1. *([11]) We assume that $f \in C^4[0,1]$ is represented by cubic B-spline wavelets as equation (2.15), where ψ has 4 vanishing moments, then*

$$|d_{j,k}| \leq \alpha\beta\frac{2^{-5j}}{4!}, \tag{4.1}$$

where $\alpha = \max|f^{(4)}(t)|_{t\in[0,1]}$ and $\beta = \int_0^1 |x^4\tilde{\psi}_4(x)|dx$.

Theorem 4.2. *([11]) Consider the previous theorem assume that $e_j(x)$ be error of approximation in V_j, then*

$$|e_j(x)| = O(2^{-4j}).$$

Thus, order of error depend on the level j. Obviously, for larger level of j, the error of approximation will be smaller.

Theorem 4.3. *([21]-[22]) For the $m-$th order B-spline wavelet the approximation error decreases with the $m-$th power of the scale 2^j,*

$$\|f - P_j f\| \leq C2^{-jm}\|f^{(m)}\|.$$

Specifically we can derive the following asymptotic relation [23],

$$\lim_{j\to\infty}\|f - P_j f\| = C_m 2^{-jm}\|f^{(m)}\|,$$

where the constant C_m is the same for all spline wavelet transforms of a given order m, and is given by

$$C_m = \sqrt{\frac{B_{2m}}{(2m)!}}.$$

where B_{2m} is Bernouilli's number of order $2m$.

In the above theorem, $\|f\|$ defined as

$$\|f\| = \left(\int_0^1 f^2(x)dx\right)^{\frac{1}{2}}.$$

Theorem 4.4. *Assume $K_1, K_2 \in L^2$ in two dimensional rectangle $[0,1]\times[0,1]$ and $g_1, g_2 \in C([0,1]\times[0,1])$. If y and y_j are the exact and approximate solution (obtained by $m-$order B-spline wavelet) of equation (1.1), respectively, then*

$$\|y(x) - y_j(x)\| \leq B2^{-jm}\|y^{(m)}\|.$$

Proof: From equation (1.1) we get

$$\|y(x) - y_j(x)\| \leq \left\| \int_0^1 K_1(x,t) \left(g_1(t,y(t)) - g_1(t,P_j y(t))\right) dt \right\| + \left\| \int_0^x K_2(x,t) \left(g_2(t,y(t)) - g_2(t,P_j y(t))\right) dt \right\|, \quad (4.2)$$

by Cauchy Schwartz inequality the first part of right hand integral can be written as

$$\left\| \int_0^1 K_1(x,t) \left(g_1(t,y(t)) - g_1(t,P_j y(t))\right) dt \right\| \leq M_1 \left(\int_0^1 \left(g_1(t,y(t)) - g_1(t,P_j y(t))\right)^2 dt \right)^{\frac{1}{2}}, \quad (4.3)$$

where

$$\left(\int_0^1 \left(K_1(x,t)\right)^2 dt \right)^{\frac{1}{2}} \leq M_1,$$

on the other hand by the mean value theorem we can write

$$g_1(t,y) - g_1(t,P_j y) \leq A_1 |y(t) - P_j y(t)|, \quad (4.4)$$

where

$$A_1 = sup\{|g_{1_2}(t,s_1(t))|, 0 \leq t \leq 1\},$$

and g_{1_2} is the derivative of g_1 respect to the second variable, also

$$\begin{aligned} &\int_0^x K_2(x,t) \left(g_2(t,y(t)) - g_2(t,P_j y(t))\right) dt \\ &\leq \int_0^x |K_2(x,t)|.|g_2(t,y(t)) - g_2(t,P_j y(t))| dt \\ &\leq M_2 \int_0^x |g_2(t,y(t)) - g_2(t,P_j y(t))| dt, \end{aligned} \quad (4.5)$$

where $M_2 = sup\{|K_2(x,t)|, 0 \leq x,t \leq 1\}$. On the other hand

$$|g_2(t,y(t)) - g_2(t,P_j y(t))| \leq A_2 |y(t) - P_j y(t)|, \quad (4.6)$$

with

$$A_2 = sup\{|g_{2_2}(t,s_2(t))|, 0 \leq t \leq 1\},$$

where g_{2_2} is the derivative of g_2 respect to the second variable. Substituting equations (4.3)-(4.6) and pervious theorem in equation (40) we get:

$$\|y(x) - y_j(x)\| \leq (M_1 A_1 + M_2 A_2) C 2^{-jm} \|y^{(m)}\|,$$

putting $B = (M_1 A_1 + M_2 A_2)C$, proof is completed. □

Proposition 4.5. *It is interesting to point out that if the functions $g_i(t,y), i=1,2$ satisfies in Lipschitz condition, that is there exist Lipschitz constants L_i, $i=1,2$ such that*

$$|g_i(t,y_1)-g_i(t,y_2)| \le L_i\,|y_1-y_2|\,, \qquad i=1,2,$$

the pervious theorem is proved easily without applying mean value theorem.

5. Illustrative example

In this section, for showing the accuracy and efficiency of the described methods we present some examples. The solution of $y_(x)$ is obtained by the methods in section 3 at the octave level $j_0=3$ and at the levels $j_u=3,4,5$ and are compared with the results of some other methods. In tables the absolute errors are defined as follows

$$\|e(y)\| = |y(x)-y^*(x)|, \qquad i=1,2,...,n,$$

where y and y^* are the exact and approximated solutions, respectively.

Example 5.1. *[13] Consider the equation*

$$y(x)=\frac{-1}{30}x^6+\frac{1}{3}x^4-x^2+\frac{5}{3}x-\frac{5}{4}+\int_0^x(x-t)(y(t)^2)dt+\int_0^1(x+t)y(t)dt, \quad (5.1)$$

with the exact solution $u(x)=x^2-2$. Table 1 presents exact and approximation solution for $u(x)$, obtained by the method in section 4 at the octave level $j_0=3$ and at the levels $j_u=3,4,5$.

R.H.F: approximated solution by rationalized Haar functions [13].

Table 1: Absolute error of approximated solution of example 5.1 in some mesh points.

	Approximate			R.H.F
x	$j_u=3$	$j_u=4$	$j_u=5$	$k=16$
0	1.06581×10^{-11}	1.13602×10^{-14}	3.40015×10^{-17}	2.57781×10^{-8}
0.1	1.11022×10^{-12}	8.77127×10^{-16}	1.40205×10^{-18}	1.99002×10^{-8}
0.2	1.77636×10^{-12}	1.99740×10^{-15}	1.30671×10^{-18}	2.30778×10^{-7}
0.3	1.99843×10^{-12}	4.03042×10^{-16}	4.45810×10^{-18}	6.11075×10^{-8}
0.4	8.88178×10^{-12}	4.50442×10^{-16}	2.89237×10^{-18}	1.12964×10^{-8}
0.5	4.44089×10^{-12}	3.11159×10^{-16}	1.55224×10^{-18}	1.56604×10^{-8}
0.6	2.22045×10^{-12}	2.23901×10^{-16}	6.66325×10^{-18}	3.41414×10^{-8}
0.7	0.56133×10^{-12}	1.33227×10^{-15}	3.33187×10^{-18}	9.00214×10^{-7}
0.8	6.66134×10^{-11}	6.76284×10^{-16}	3.10862×10^{-17}	3.71096×10^{-8}
0.9	0.00556×10^{-11}	0.00970×10^{-18}	9.21414×10^{-20}	8.88241×10^{-9}
1	0.01048×10^{-12}	3.10862×10^{-15}	2.96970×10^{-18}	5.10047×10^{-8}

Example 5.2. *[9] Consider the following Hammerstein mixed integral equation*

$$y(x) = x - (9e - 24)\, x^4 - \frac{x^{10}}{4} + \int_0^x x^6 t(y(t))^2 dt + \int_0^1 (xt)^4 e^{y(t)} dt, \tag{5.2}$$

with the exact solution $y(x) = x$. Table 2 presents exact and approximation solution for $y(x)$, obtained by the method in section 4 at the octave level $j_0 = 3$ and at the levels $j_u = 3, 4, 5$.

Table 2: Absolute error of approximated solution of example 5.2 in some mesh points.

	Approximate			method of [13]
x	$j_u = 3$	$j_u = 4$	$j_u = 5$	$N = 40$
0	4.75751×10^{-10}	1.00613×10^{-14}	1.13671×10^{-17}	4.26507×10^{-9}
0.1	3.66244×10^{-12}	8.88178×10^{-16}	9.07992×10^{-18}	4.78324×10^{-10}
0.2	4.05714×10^{-11}	1.99841×10^{-15}	6.00290×10^{-18}	3.54412×10^{-10}
0.3	5.33248×10^{-12}	4.44077×10^{-16}	2.84681×10^{-17}	2.07448×10^{-10}
0.4	1.94287×10^{-12}	2.24411×10^{-16}	2.34385×10^{-18}	8.89832×10^{-10}
0.5	3.23034×10^{-12}	1.33202×10^{-16}	6.46881×10^{-18}	1.49235×10^{-10}
0.6	6.90763×10^{-12}	6.55246×10^{-16}	1.15758×10^{-18}	8.91652×10^{-11}
0.7	7.01489×10^{-11}	3.10862×10^{-15}	2.27790×10^{-19}	3.17143×10^{-10}
0.8	7.15560×10^{-12}	5.38140×10^{-16}	8.78201×10^{-18}	6.58024×10^{-10}
0.9	8.31266×10^{-14}	9.11465×10^{-18}	3.77429×10^{-18}	5.80147×10^{-10}
1	2.77863×10^{-12}	4.11379×10^{-15}	5.95221×10^{-17}	3.06546×10^{-9}

Example 5.3. *Consider the following nonlinear Volterra-Fredholm integral equation*

$$y(x) = f(x) + \int_0^x x \cos(t) e^{y(t)} dt + \int_0^1 x^2 (\sec(t) - \tan(t)) \ln(y(t) + 1) dt,$$

where

$$f(x) = \sin(x) - x e^{\sin(x)} - x^2 \ln(\sin(x) + 1),$$

and the exact solution is $y(x) = \sin(x)$. Table 3 presents exact and approximation solution for $y(x)$, obtained by the method in section 4 at the octave level $j_0 = 3$ and at the levels $j_u = 3, 4, 5$.

Table 3: Absolute error of approximated solution of example 5.3 in some mesh points.

	Approximate			Method of [9]
x	$j_u = 3$	$j_u = 4$	$j_u = 5$	$N = 40$
0	3.04287×10^{-6}	2.44521×10^{-8}	1.51481×10^{-11}	2.46125×10^{-4}
0.1	1.95598×10^{-6}	2.89498×10^{-8}	2.53926×10^{-10}	6.71201×10^{-4}
0.2	2.88767×10^{-6}	3.42211×10^{-8}	6.24372×10^{-10}	3.81486×10^{-4}
0.3	1.59772×10^{-6}	4.82214×10^{-8}	9.45887×10^{-10}	3.78134×10^{-4}
0.4	3.45769×10^{-6}	6.60250×10^{-9}	9.28540×10^{-10}	3.60240×10^{-4}
0.5	8.80046×10^{-6}	1.71297×10^{-7}	2.59991×10^{-10}	8.23781×10^{-4}
0.6	8.69603×10^{-6}	4.73955×10^{-8}	8.47478×10^{-10}	4.70605×10^{-4}
0.7	4.46514×10^{-6}	1.22893×10^{-7}	1.60627×10^{-10}	4.66149×10^{-4}
0.8	6.60243×10^{-7}	2.19079×10^{-7}	1.58502×10^{-11}	1.10355×10^{-4}
0.9	8.82928×10^{-6}	9.74502×10^{-8}	1.06722×10^{-10}	1.81691×10^{-4}
1	1.71244×10^{-5}	7.17162×10^{-8}	2.63742×10^{-9}	1.18294×10^{-3}

6. Conclusions

In this paper, we proposed an advanced numerical model in solving nonlinear Fredholm-Volterra Hammerstein integral equation of the second kind by means of semi orthogonal compactly supported spline wavelets via operational matrices of these wavelets and Galerkin method. Because of some properties of B-spline wavelets such as semiorthogonality, having compact support and vanishing moments, the operational matrices of the method is so sparse (as operational matrix of product in section 2, $H_{16\times 16}$) and therefore the purposed approach cause to significant reduction in memory requirement and computational time in the programming of method. On the other hand, as we can see in examples, in comparison with some other methods, the introduced method has good accuracy. The approach can be extended to nonlinear integro-differential equation with little additional work.

Acknowledgments

The author would like to thank the anonymous reviewers of this paper for their careful reading, constructive comments and nice suggestions which have improved the paper very much.

References

1. Tricomi, F. G., *Integral Equations*, Dover, (1982).
2. Agarwal, R. P., O'Regan, D., Wong, P. J. Y., *Positive Solutions of Differential, Difference and Integral Equations*, Kluwer Academic, Dordrecht, (1999).
3. Ibragimov, N. H., Ibragimov, R. N., *Invariant solutions as internal singularities of nonlinear differential equations and their use for qualitative analysis of implicit and numerical solutions*. Communications in Nonlinear Science and Numerical Simulation 14, 3537-3547, (2009).
4. O'Regan, D., Meehan, M., *Existence Theory for Nonlinear Integral and Integro-differential Equations*, Kluwer Academic, Dordrecht, (1998).

5. Banas, J., Rzepka, V., *On existence and asymptotic stability of solutions of a nonlinear integral equation*. J. Math. Anal. Appl. 284, 165-173, (2003).

6. Paripour, M., Kamyar, M., *Numerical solution of nonlinear Volterra-Fredholm integral equations by using new basis functions*. Communication in Numerical Analysis 2013, 1-11, (2013).

7. Ahmadabadi, M. N., Dastjerdi, H. L., *A numerical solution of mixed Volterra-Fredholm integral equations of Uryshon type on non-rectangular regions using meshless methods*. Journal of Linear and Topological Algebra 4 (4), 289-304, (2015).

8. Rabbani, M., Jamali, R., *Solving nonlinear system of Volterra-Frdholm integral equations by using variational iteration method*. Journal of Mathematics and Computer Science 5(4), 280-287, (2012).

9. Hashemizadeh, E., Rostami, M., *Numerical solution of Hammerstein integral equations of mixed type using the Sinc-collocation method*. Journal of Computational and Applied Mathematics 279, 31-39, (2015).

10. Hadizadeh, H., Asgary, M., *An efficient numerical approximation for the linear class of mixed integral equations*. Appl. Math. Comput. 167, 1090-1100, (2005).

11. Maleknejad, K., Nouri, K., Nosrati Sahlan, M., *Convergence of approximate solution of nonlinear Fredholm-Hammerstein integral equations*. Commun. Non. Sci. Num. Simul. 15 (6), 1432-1443, (2010).

12. Maleknejad, K., Nosrati Sahlan, M., *The method of moments for solution of second kind Fredholm integral equations based on B-spline wavelets*. International Journal of Computer Mathematics 87, 1602-1616, (2010).

13. Ordokhani, Y., Razzaghi, M., *Solution of nonlinear Volterra-Fredholm Hammerstein integral equations via a collocation method and rationalized Haar functions*. Applied Mathematics Letters 21, 4-9, (2008).

14. Chui, C., *An introduction to wavelets*, New york: Academic press, (1992).

15. Daubechies, I., *Ten lectures on wavelets*, Philadelpia, PA; SIAM, (1992).

16. Strang, G. and Nguyen, T., *Wavelets and filter banks*, Cambridge, MA: Wellesley-Cambridge, (1997).

17. Telesca, L., Hloupis, G., Nikolintaga, I., Vallianatos, F., *Temporal patterns in southern Aegean seismicity revealed by the multiresolution wavelet analysis*. Commun. Nonl. Sci. Num. Simul. 12, 1418-1426, (2007).

18. Chui, C., *Wavelets: a mathematical tool for signal analysis*, Philadelpia, PA: SIAM, (1997).

19. Mallat, S. G., *A theory for multiresolution signal decomposition: The wavelet representation*. IEEE Trans, Pattern Anal. Mach. Intell. 11, 674-693, (1989).

20. Nosrati Sahlana, M., Hashemizadeh, E., *Wavelet Galerkin method for solving nonlinear singular boundary value problems arising in physiology*. Applied Mathematics and Computation 250, 260-269, (2015).

21. Strang, G., *Wavelets and dilation equations: a brief introduction*. SIAM Review 31, 614-627, (1989).

22. Strang, G. and Fix, G., *A Fourier analysis of the finite element variational method, in: Constructive Aspect of Functional Analysis*. Edizioni Cremonese, Rome, 796-830, (1971).

23. Unser, M., it Approximation power of biorthogonal wavelet expansions. IEEE Trans. Signal Processing 44 (3), 519-527, (1996).

24. Kalman, R. E., Kalaba, R. E., *Quasilinearization and Nonlinear Boundary-Value Problems*, Elsevier, New York, (1969).

M. Nosrati Sahlan
Department of Mathematics and Computer Sciences,
University of Bonab, 55517-61167, Bonab, Iran.
E-mail address: nosrati@bonabu.ac.ir